Abnormal Myocardial and Coronary Vasculature Development in Experimental Hypoxia

ONDREJ NANKA,[1]* PETRA KRIZOVA,[1] MICHAL FIKRLE,[1] MICHAL TUMA,[1] MILAN BLAHA,[2] MILOS GRIM,[1] AND DAVID SEDMERA[1,2]

[1]Institute of Anatomy, Laboratory of Molecular Embryology, First Faculty of Medicine, Charles University, Prague, Czech Republic
[2]Institute of Animal Physiology and Genetics, Laboratory of Cardiovascular Morphogenesis, Academy of Sciences of the Czech Republic, Czech Republic

ABSTRACT

Oxygen availability is one of the necessary prerequisites for normal embryonic development. In our previous study we found that quail embryos incubated under hypoxic conditions (16% O_2) die at embryonic day (ED) 9 with signs of heart failure. By ED4 and ED6 we found thinner ventricular wall and increased capillary density. We thus hypothesized that the cause of death would lie in severe myocardial and coronary maldevelopment. ED6 and 7 hypoxic hearts had thinner ventricular wall, especially left. There was a simultaneous increase in capillary density, most pronounced in the interventricular septum. This site corresponds to an area of tissue hypoxia and ensuing increased angiogenesis, and also formation of ventricular conduction system. Hypoxia had a positive effect on normal sequence of maturation of the conduction system evaluated by optical mapping at ED7. In sections from ED9 hypoxic hearts we found, in addition to thinner ventricular walls, irregularities in development of coronary tree (missing coronary ostia, absence of one coronary artery, and irregular arterial wall). This deficiency was due to decreased myocyte proliferation rather than to increased apoptosis. By Indian ink injection through the left ventricle we found in normoxic hearts regular coronary branching pattern, while in the hypoxic ones there was often only an irregular plexus. Embryonic hypoxia thus leads to increased capillarity and trabeculation to minimize diffusion distance. In the subsequent period there is a failure in organization of vascular plexus into normal vasculature, resulting in thin compact myocardium that likely leads to heart failure and embryonic death. Anat Rec, 291:1187–1199, 2008. © 2008 Wiley-Liss, Inc.

Key words: quail embryo; vasculogenesis; coronary artery; proliferation

*Correspondence to: Ondrej Nanka, Institute of Anatomy, First Faculty of Medicine, U Nemocnice 3, 128 00 Prague 2, Czech Republic. Fax: +420-2-2496-5770.
E-mail: ondrej.nanka@ lf1.cuni.cz

INTRODUCTION

Although vertebrate embryogenesis occurs in rather hypoxic environment in comparison with adults, oxidative metabolism is necessary for proper cellular function and embryonic survival. Both lack and surplus of oxygen are deleterious for normal development, and oxygen tension is tightly regulated in the embryo (Webster and Abela, 2007). Mammalian embryos are fairly well equipped to survive short periods of hypoxia or anoxia, but even such brief exposures can cause a spectrum of developmental defects (transverse limb reductions, face and heart malformations; reviewed in Webster et al., 2007). Hypoxia is a stimulus for both embryonic and adult angiogenesis, and together with hemodynamics the main factor directing development and patterning of the cardiovascular system (Ribatti, 2006). Improved understanding of the underlying molecular mechanisms of hypoxia-triggered signaling can have potential therapeutic implications in various disease states.

The early stages of cardiac development occur in the absence of coronary vasculature, but establishment of coronary perfusion is necessary for ventricular compaction that enables increased pumping efficiency of the fetal heart (Rychter and Ostadal, 1971; Rychterova, 1971; Sedmera et al., 2000). During this process, the sponge-like ventricular myocardium that takes its nutrition from the ventricular lumen is transformed into a compact structure, nourished from the outside by the means of coronary arteries. Deficient coronary development precludes compaction and is the basis of embryonic lethality in mice lacking coronary arteries (Kwee et al., 1995); reviewed in (Wessels and Sedmera, 2003), or, when localized, could be a cause of recently recognized noncompacted cardiomyopathy (Varnava, 2001). Molecular mechanisms orchestrating coupled development between myocardium and coronary vasculature were recently summarized by Bhattacharya et al. (2006), whereas current views on the genetic pathways controlling development of the coronary vasculature were reviewed by Olivey et al. (2004). However, recent experimental study by Lavine et al. (2008) have pointed out that regulation of cell proliferation in myocardium and coronary vasculature utilizes genetically distinct pathways.

Coronary arteries are derived from the epicardium, which itself originates from the proepicardial organ (Viragh et al., 1993). The subepicardial layer is generated by the process of epithelial to mesenchymal transformation, followed by invasion of these cells into myocardium where they form coronary vessels and cardiac fibroblasts (Vrancken Peeters et al., 1999). Primitive vascular plexus is then established, and remodeling into morphologically distinct arteries and veins occurs after its connections to the aorta (Tomanek et al., 2006b).

Apart from genetic factors, environmental influences play an important part in morphogenesis. From those, one of the most pronounced epigenetic factors influencing vasculogenesis is hypoxia (Ribatti, 2006). Effects of hypoxia on cardiac development were studied for some time (Jaffee, 1978; Rouwet et al., 2002; Sharma et al., 2006). Recently, regional differences in myocardial tissue oxygenation during development were described (Wikenheiser et al., 2006), and regions with the lowest oxygen availability in the myocardium of the atria and interventricular septum were correlated with known sites of for-

mation of coronary vessel and pacemaking and conduction system.

In this study, we sought to characterize in detail the hypoxia-induced myocardial phenotype (Nanka et al., 2006) and clarify the cellular mechanisms leading to it. We found that decreased oxygen availability caused the thin compact myocardium phenotype with increased trabeculation and vasculogenesis, and accelerated maturation of ventricular activation sequence. The defect in ventricular compact layer thickness was a result of decreased myocyte proliferation, rather than increased apoptosis. Ultimately, the vascular plexuses failed to undergo normal connection to the aorta and remodeling, preventing ventricular compaction and leading to heart failure and embryonic demise.

MATERIAL AND METHODS

Egg Incubation

The effect of hypoxia on embryonic angiogenesis was studied in embryos of Japanese quail (Coturnix coturnix japonica) from ED 5 to ED9, that is, at HH stages 26–27 and 37 (Hamburger and Hamilton, 1951). Fertilized eggs were incubated at 38°C and 60%–85% humidity under normoxic (21 kPa, 21% O_2) conditions for the first 48 hr and subsequently for 48–168 hr under hypoxic (16 kPa, 16% O_2) conditions. After the first 48 hr, the nonfertilized eggs (on average 10%) were discarded, and from there on, the survival was checked daily. The oxygen concentration in the hypoxic incubator was calibrated by platinum electrode. Controls were incubated in normal atmospheric oxygen tension. The temperature was the same in both incubators.

Detection of Tissue Hypoxia

Hypoxyprobe 1 (pimonidazol hydrochloride, Natural Pharmacia International, Inc., Research Triangle Park, NC) has been used according to recommendation of the producer and our protocol (Nanka et al., 2006). After intravenous administration it is evenly distributed throughout the embryo. Hypoxyprobe-1 (30 μg/100 mg in phosphate buffer saline [PBS]) was injected in the vitelline (chorioallantoic) vein at ED6 or 8 (HH 30 or 35, number of embryos in normoxic group = 8, in hypoxic group = 7). Embryos were reincubated for 1 hr and fixed in 4% paraformaldehyde in PBS. The reaction product was detected on paraffin sections with Hypoxyprobe-1 monoclonal antibody (1:50) for 40 min at room temperature (RT) and the secondary antibody conjugated with alkaline phosphatase (1:300) for 1 hr at RT. The color reaction was visualized by nitroblue tetrazolium (NBT)/ Xphosphate. The sections from control and experimental reaction were incubated in parallel in one reaction for the same time. The pictures were taken by the same camera (Olympus DP50) with identical exposure settings.

Hematoxylin and Eosin Staining

Paraffin sections were mounted on silane-coated slides and rehydrated through Histoclear and a series of graded ethanols. Next, the slides were dipped in Harris Hematoxylin (Sigma, stains negatively charged nucleic acids purple) for ∼ 2 min followed by a quick dip in a solution of 70% ethanol and 1 N HCl for nuclear differen-

tiation. The slides were then placed in ammonium hydroxide for ~1 min followed by rinsing in water to turn the purple color blue. The slides were then dipped in Eosin Y (Sigma, stains cytoplasmic proteins pink) for ~1 min and subsequently dehydrated through a series of graded ethanols and cleared in xylene. Slides were finally coverslipped with Depex mounting medium (Electron Microscopy Sciences) and examined on an Olympus BX51 compound microscope.

Immunohistochemistry on Paraffin Sections

Embryos were collected at appropriate stages (HH 26 – 8 normoxic and 6 hypoxic embryos; HH32 – 9 normoxic and 6 hypoxic embryos; HH 37 – 8 normoxic and 7 hypoxic embryos), fixed in Dents fixative (80% methanol/20% dimethylsulfoxide [DMSO]), and prepared for Paraplast embedding and sectioning. Primary antibodies used were QH1 at 1:1,000 (Developmental Studies Hybridoma Bank, University of Iowa). This antibody stains quail vascular endothelial cells and haemopoietic cells (Pardanaud et al., 1987). Alpha-smooth muscle actin (SMA) monoclonal antibody (Sigma, A2547) was used to visualize tunica media layer of coronary arteries at 1:500 dilution. Secondary antibody (Peroxidase-conjugated Goat anti mouse; Sigma: A4416, diluted 1:200) was applied for 90 min at RT and staining was revealed by the diaminobenzidine color reaction. For fluorescent labeling of nascent ventricular conduction system we used HNK1 and PSA-NCAM antibodies at 1:100 dilution as described (Chuck and Watanabe, 1997; Sedmera et al., 2004).

Indian Ink Injections

Embryos at ED8 and ED9 were used for the injection of Indian ink into the left ventricle (HH 35 – 10 normoxic and 10 hypoxic embryos; HH 37 – 10 normoxic and 10 hypoxic embryos). The embryos were removed from the eggs and transferred to a dish with Locke's salt solution. To have the heart accessible for injection, midline thoracotomy was performed with iridectomy scissors. After that, solution of Indian ink diluted in PBS (1:5) was slowly injected into the left ventricle. Injections were performed using sharpened glass micropipettes (diameter of 10 to 20 µm). Following ink injection, the hearts were removed from the embryos and fixed for at least 24 hr in Serra's fixative solution. After clearing the specimens in glycerin, the coronary vasculature of each heart was studied under a dissecting microscope.

Whole Mount Immunostaining

Embryonic hearts from ED8 and 9 were fixed for 24 hr in Dents fixative solution (HH 35 – 10 normoxic and 10 hypoxic embryos; HH 37 – 10 normoxic and 10 hypoxic embryos). The reaction started with washing in PBS and the hearts were preblocked in 5% goat serum in PBS, and then incubated for 24 hr with anti-SMA antibody (1:500, Sigma, A2547) at RT on rotating wheel. Extensive washes in PBS (3 × 30 min) were followed by 4 hr incubation with secondary goat anti mouse tetramethylrhodamine isothiocyanate (TRITC) IgG antibody (Jackson Lab, 1:100) in PBS at RT. Before examination under a fluorescence dissecting microscope (Olympus SZX 12, Japan), the hearts were stored at 70% ethanol.

Optical Mapping of Ventricular Activation

Isolated beating embryonic hearts between ED3 and ED7 were stained with voltage-sensitive dye (Di-4-ANEPPS, Calbiochem) and imaged at 37°C with Ultima L high-speed camera (SciMedia Ltd., Japan) at 1 kHz. The protocol and processing algorithms for generation of activation maps were described in detail previously (Reckova et al., 2003). The number imaged at each developmental stage and condition was at least five.

Bromodeoxyuridine Pulse Labeling and Immunohistochemistry

Two hours before sacrifice, the embryos (HH 27 – 3 normoxic and 5 hypoxic, HH 30 – 5 normoxic and 5 hypoxic; HH 32 – 3 normoxic and 3 hypoxic) were labeled at ED 5, 6, and 7 with a saturating dose of 50 µg of bromodeoxyuridine (BrdU) (Sigma) in 200 µL of Tyrone's saline applied directly over the vascular bed (Sedmera et al., 2002a). The embryos were then fixed in Dent's fixative and processed into paraffin. Serial transverse sections were cut at 10 µm and mounted on silane-coated slides (Sigma). Histological analysis was performed using a triple staining protocol for sarcomeric actin (1:1,000, Sigma) as a myocyte marker, BrdU (1:100, BD Biosciences) for S-phase nuclei, and DRAQ 5 (1:1,000, Biostatus Limited, UK) for all nuclei. The sections were examined on a Leica TCS SP2 AOBS confocal microscope. Fields from the left and right ventricular free wall, that is, the same layer where apoptosis, capillary density, and compact layer thickness were measured at ventricular midportion, were recorded using a 40× oil immersion lens at 1,024 × 1,024 pixel resolution. The area of the interventricular septum was not analyzed, since there are significant regional differences in cell proliferation due to presence of slowly dividing conduction tissues (Cheng et al., 1999). Similarly, no measurements were done in the trabecular layer, which presents a strong inside to outside gradient of proliferation (Sedmera et al., 2002a). The final images were maximum intensity projections of six optical sections, 1 µm apart collapsed using Leica software to produce a single projection image. Cells were counted in Adobe Photoshop 7.0 (Adobe Systems Inc., San Jose, CA), where black dots were placed in separate layers over the nuclei, then transferred for automated counting to ImageJ (freeware, National Institutes of Health, Bethesda, MD). The number of BrdU-positive nuclei per tissue volume was then calculated from known field area (275 × 275 µm^2) and 5 µm z-dimension.

Detection of Apoptosis on Whole Mounts—LysoTracker Red Staining

Stock solutions (50 µL) of 1 mM LTR (Molecular Probes, Eugene, OR) in DMSO were diluted in 20 mL of PBS (Schaefer et al., 2004). The embryos on ED 7 (HH 32 – 11 normoxic and 14 hypoxic embryos) were dissected to expose the heart and incubated in the Lyso-Tracker Red (LTR) solution for 15 min at RT while rocking and washed in PBS before fixation. The embryos were fixed in 4% paraformaldehyde in PBS over night at 4°C, rinsed in PBS, and stored at 4°C before observation and further processing (paraffin sections and nuclear counterstaining with 4′, 6-diamidino-2-phenylindole [DAPI]).

Immunostaining for Apoptosis

To confirm the patterns of distribution of apoptotic cells from whole mount reaction, immunofluorescence was performed on serial sister sections from hearts used for immunohistochemistry using a rabbit polyclonal antibody, antiactive caspase 3 (1:1,000, BD PharMingen) detected by Cy-3 coupled secondary (1:100, Jackson Immuno). The sections were then counterstained with Hoechst 33258 (1:10,000, Sigma) nuclear dye, dehydrated, and coverslipped with Depex mounting medium (Electron Microscopy Sciences). Cell counting was performed in the same area where proliferation, capillary density, and compact layer thickness were measured, that is, lateral free wall of both ventricles at ventricular midportion.

Quantitative Measurements and Statistical Analysis

Compact layer thickness was measured on images acquired on Olympus BX51 microscope equipped with DP70 digital camera using Cell P software (Soft Imaging System GmbH) with Measure function. We measured thickness of the compact myocardium on corresponding sites (transverse section, H&E staining, ventricular midportion, lateral wall) in both right and left ventricle. Details of quantification of proliferation and cell death rates are given above under respective headings. The percentage of capillaries was measured on sister sections stained with QH1 antibody acquired with $40\times$ objective. We defined the region of compact myocardium and measured the surface area of capillaries and myocardium by Cell P analyzing software. That was achieved by using a grid of 10×10 μm^2 and counting the number of intercepts with QH1-positive cells (or areas enclosed by them, i.e., the lumen) and the remaining tissue. At stages below ED7, only capillaries were present in the myocardium; on ED9, areas containing larger vessels (e.g., septal artery in the interventricular septum) were avoided to prevent possible confusion with venules. Typically, larger caliber vessels were present only in the subepicardial space, which was not subject of this evaluation.

For analysis of presence of coronary arteries we used hearts stained in whole mount by SMA antibody. At ED9, this staining labeled the coronary stems and main branches that already acquired smooth muscle coat (Tomanek et al., 2006a) allowing unambiguous detection of number and connections of the coronaries. Additional information on the vascular plexuses was obtained from Indian ink injected specimens.

All data are shown as mean ± SD. Statistical comparison of differences between groups was performed by using an unpaired two-tailed Student's t test. For comparison of regions within the same heart, a paired t test was used. Chi-Square test was used where appropriate (optical mapping data). Differences between groups were considered significant at $P < 0.05$.

RESULTS

Survival in Hypoxia and Hypoxic Areas in the Heart

Under hypoxia (16% O_2), the embryonic survival was considerably reduced in comparison with normoxic con-
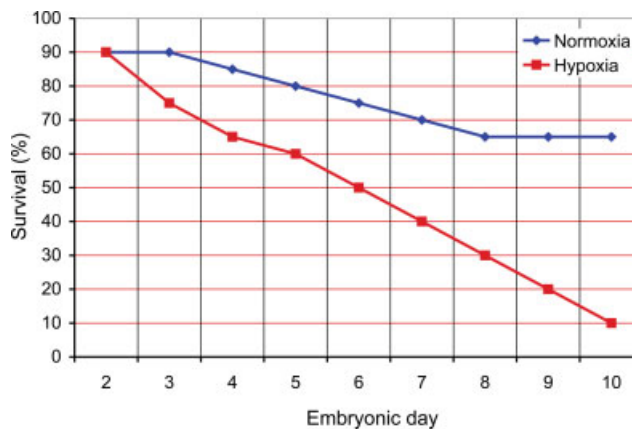

Fig. 1.   Survival of quail embryos under normoxic and hypoxic conditions. The values are based on a total number of 150 embryos incubated under normoxic conditions and 200 under hypoxic conditions. At ED9 (stage 37), most of the hypoxic embryos are dead, and only 10% survive to ED10 (stage 38).

ditions (Fig. 1), with almost no embryos alive after ED10. Analysis of hypoxia at the tissue level showed most intense staining in the thickest parts of the myocardium, that is, left ventricular compact layer, interventricular septum, atrioventricular canal, and outflow tract myocardium. There was an increase in the extent of hypoxic areas under hypoxic conditions at ED6 (stage 30) and 8 (stage 35/36; Fig. 2), with staining detected also in the left ventricular trabeculae, and the compact layer thickness was clearly decreased. This finding prompted us to further analyze the phenotype by quantification of this parameter at different stages of development.

Abnormal Myocardial and Coronary Artery Development in Hypoxia

Indeed, the ventricular compact layer was found to be significantly thinner than in controls (Fig. 3), which might present an adaptive mechanism for decreasing diffusion distance. However, thickness of both left and right ventricular compact layer increased between stages also under hypoxia, albeit at slower pace.

By systematic scanning of serial sections from hearts sampled at ED9 (stage 37), we noted there were also problems with the coronaries that were often irregularly formed or missing (Figs. 4 and 5). To confirm and quantify the involvement, Indian ink injection into the left ventricle (Fig. 6) with whole mount SMA staining (Fig. 7) was performed. It was found that only 20% of hypoxic hearts showed normal pattern of connection of the coronary arteries to the aorta (Table 1).

Increased Capillary Density in Hypoxic Hearts

Interestingly, but perhaps not surprisingly in the light of our previous work showing increased vascular endothelial growth factor (VEGF) expression under hypoxic conditions (Nanka et al., 2006), there was significantly increased capillary density in the interventricular septum at ED5, 7, and 9 (+57%, +63%, and +65%, respectively). The difference was somewhat less pronounced in
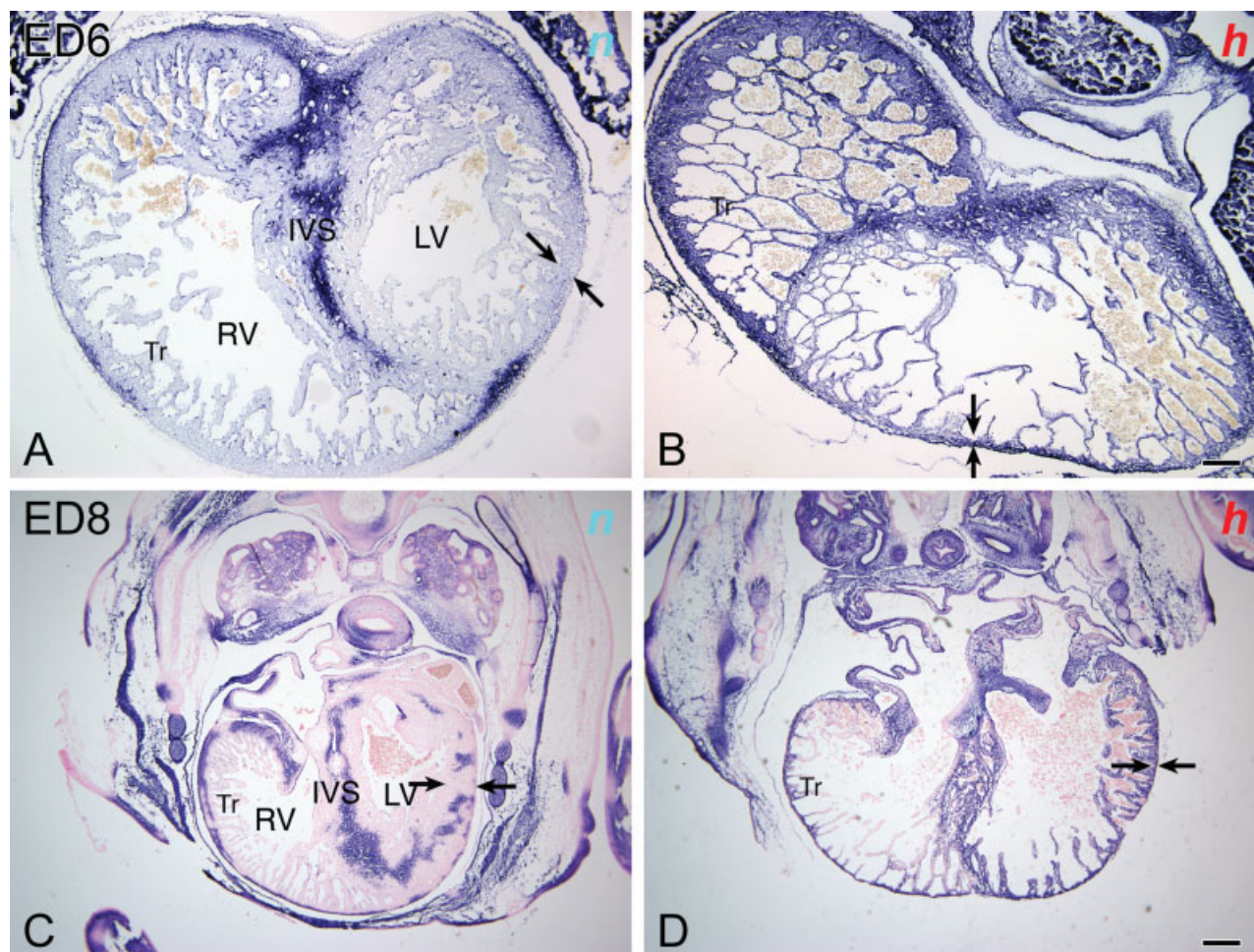
Fig. 2. Tissue hypoxia in normoxic (n) and hypoxic (h) embryos at ED6 (stage 30) and ED8 (stage 35). Sections of heart ventricles are stained with Hypoxyprobe-1. **A, B**: Transverse sections through ventricles at ED6. Tissue hypoxia is detected in ventricular wall and interventricular septum (IVS) of the normoxic specimen (A). In the hypoxic embryo (B), hypoxic areas are larger and include both compact myocardium and trabeculae. Note increased and finer trabeculation (Tr) of the hypoxic myocardium. LV, left ventricle, RV, right ventricle. Scale bar = 100 μm. **C, D**: Sections through ventricles at ED8. Tissue hypoxia is detected in ventricular wall and interventricular septum of the normoxic specimen (C). In the hypoxic embryo (D), areas under hypoxia are larger and include both compact and trabecular myocardium. Note the thin compact myocardium and richer trabeculation (Tr) in the hypoxic heart. Arrows show the measurements of compact layer thickness (lower under hypoxia). Scale bar = 250 μm.

the ventricular free wall, with the increase being significant in the left ventricle only at ED7 (stage 31) and 9 (stage 37), and in the right ventricle at ED9 only (Fig. 8).

The capillary density in the interventricular septum was higher than in the ventricular free wall in both normoxic and hypoxic embryos. This site corresponds to an area of maximal tissue hypoxia (Fig. 2) and ensuing vasculogenesis.

Effect of Hypoxia on Conduction System Maturation

The interventricular septum is also site of conduction system formation, correlating with hypoxic regions (Wikenheiser et al., 2006). The functionality of conduction system can be inferred from optical mapping of epicardial activation patterns (Reckova et al., 2003; Sedmera et al., 2006). Epicardial activation maps detailed

the sequence of ventricular activation, which was in many respects similar to that reported previously in the chick (Reckova et al., 2003; Sedmera et al., 2004). At ED3 (stages 16/17), left-to right, base-to-apex activation was observed on the anterior ventricular surface in all six hearts examined, with preferential conduction pathway along the primordium of the interventricular septum posteriorly present in two. At ED4 (stages 22-24), two out of 9 hearts examined showed already apex-to-base activation, and anterior preferential conduction pathway (Fig. 9B) was noted in four. The rest showed base-to-apex, left-to-right sweep of activation like the earlier stages. At ED5 (stages 27/28), apex-to-base activation was present in four out of 18 hearts examined (22%); at ED6 (stage 29/30), this proportion rose to 25% (N = 16), and 32% at ED7 (stage 31; N = 19). There was no significant difference in frequency of apex-to-base activation pattern between normoxic and hypoxic

hearts (Fig. 9) at ED5 (30% apex-to-base in hypoxic, N = 10) or ED6 (20%, N = 5) but apex-to-base activation was present in all 8 hypoxic hearts examined at ED7 (stage 31; $P = 0.008$, Chi-square test). Likewise, no differences were spotted in the location of atrial pacemaker (Sedmera et al., 2006), which was shown previously to colocalize with region of increased tissue hypoxia in the

vicinity of sinoatrial nodal artery (Wikenheiser et al., 2006). Immunohistochemical examination of the hearts did not reveal any remarkable differences between normoxic and hypoxic hearts; HNK1, marker for neural crest that stains the proximal part of the ventricular conduction system (Chuck and Watanabe, 1997) showed normal expression, whereas the PSA-NCAM antibody did not react with quail tissue using protocol with paraffin sections, but stained identically processed chick tissue that served as a positive control (data not shown).

Cellular Mechanisms of Abnormal Ventricular Wall Development

We sought next to clarify the mechanism leading to thin compact myocardium phenotype. Proliferation of normoxic and hypoxic ventricular cardiomyocytes in quail was analyzed after 2 hr bromodeoxyuridine labeling at ED5, 6, and 7. There was a gradual decrease in proliferation in both ventricles with advancing development. Proliferation was decreased under hypoxic condition. On ED6 (stages 29/30), there were $68.45 \pm 18.22 \times 10^6$ positive cells per mm^3 of ventricular wall in the normoxic right ventricle versus $42.07 \pm 1.30 \times 10^6$ per mm^3 in the hypoxic right ventricle (mean $\pm$ SD, $P = 0.025$), and $59.81 \pm 11.08 \times 10^6$ per mm^3 versus $37.44 \pm 18.30 \times 10^6$ per mm^3 in the left ventricle ($P = 0.035$). Similar decrease was noted on ED5 and ED7, but below statistical significance ($P > 0.05$).

To assess the relative contribution of cell death to observed phenotype, whole mount supravital staining was performed in ED7 (stage 31) isolated hearts with Lysotracker Red (Schaefer et al., 2004). We observed
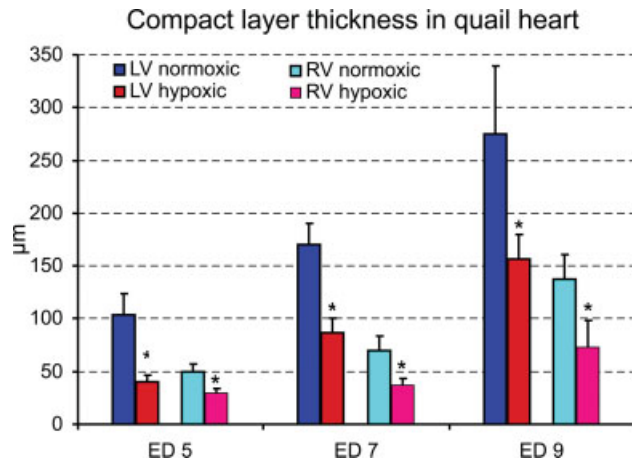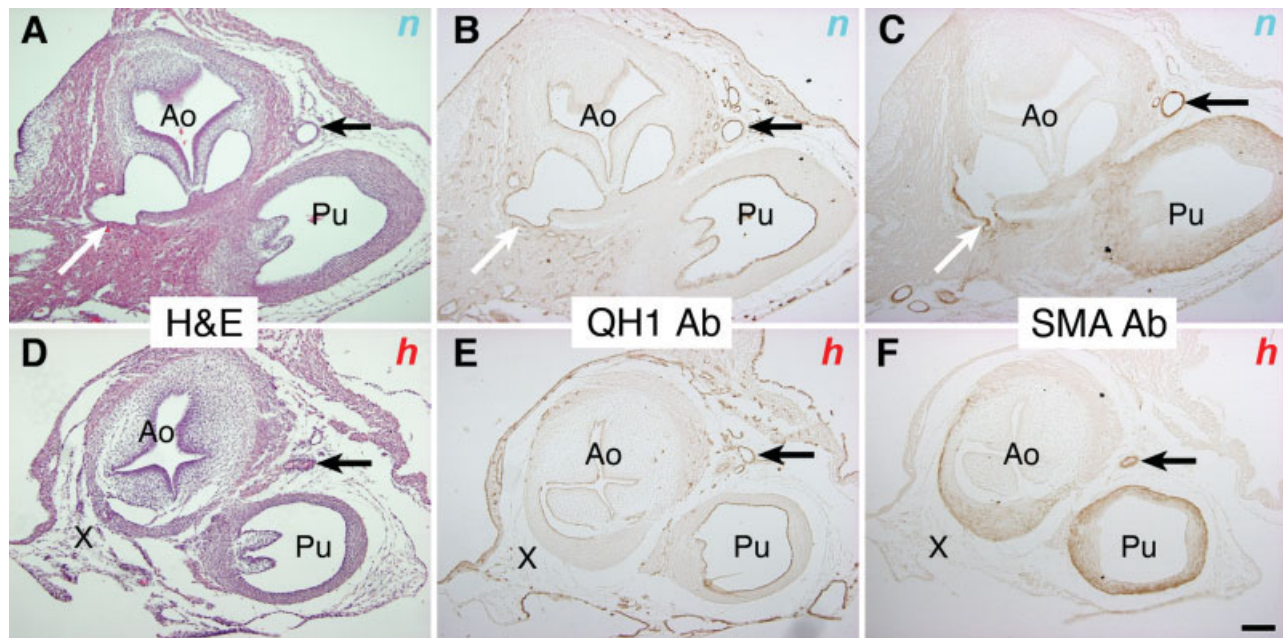

Fig. 3. Ventricular compact layer thickness in quail hearts. Compact myocardium is thinner under hypoxia in both ventricles, with more pronounced difference in the left one which is normally thicker. Developmental increase in thickness is slower in the hypoxic hearts. Mean $\pm$ SD, *$P < 0.05$ (t test). EDs 5, 7, and 9 correspond to Hamburger-Hamilton stages 26/27, 31/32, and 37, respectively.

Fig. 4. Coronary anomalies in hypoxic hearts. **A–C**: Outflow tract of ED 9 (stage 37) normoxic heart stained with H&E (A), QH1 (**B**), and SMA (C). The white arrows show the position of the right coronary artery and the black arrows the ostium of the left coronary artery. **D–F**: Black arrow points to the position of left coronary artery, the right coronary artery is missing (X) in this case. Ao, aorta; Pu, pulmonary artery. Scale bar = 100 μm.
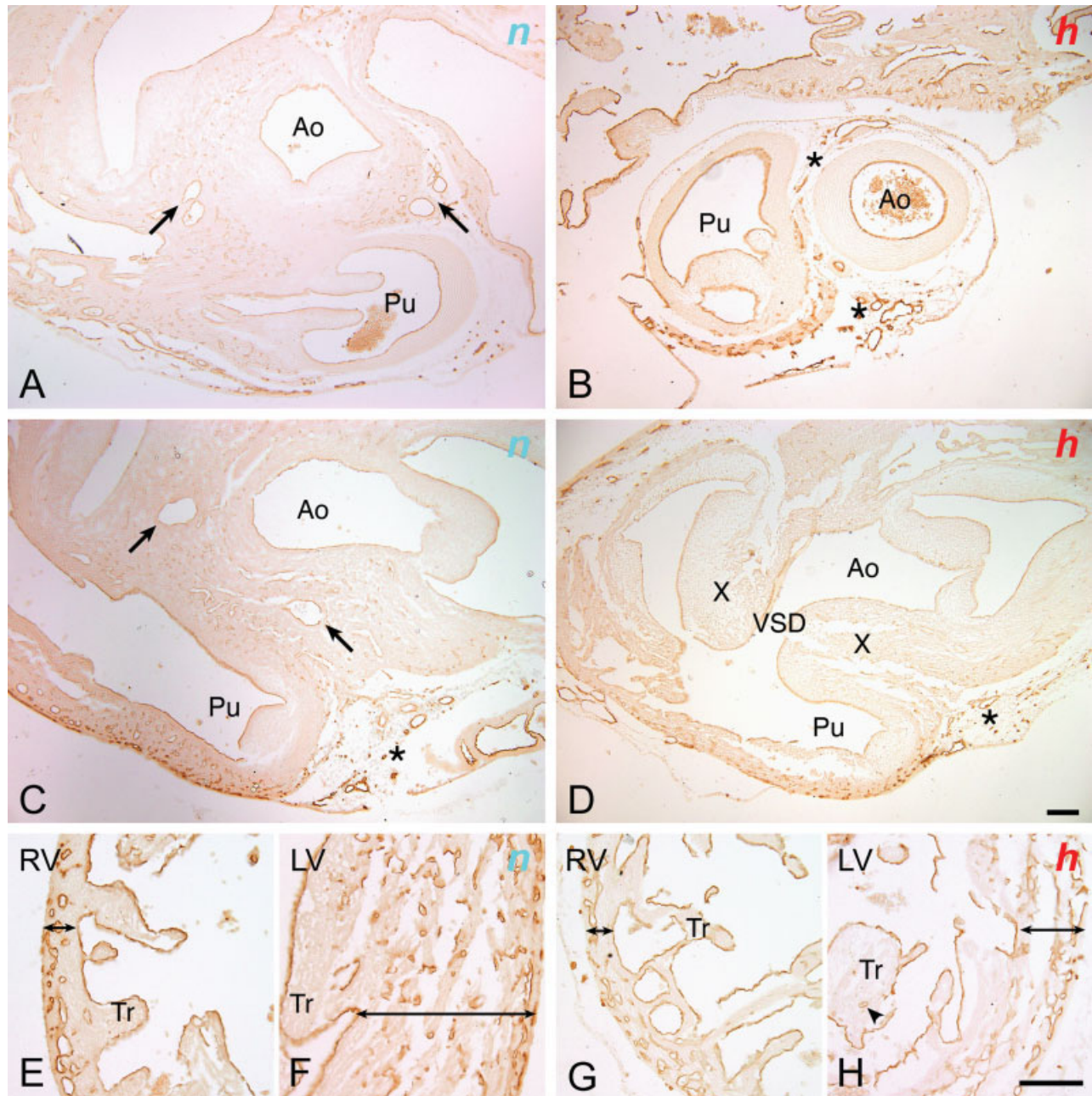
Fig. 5. Rich vascular plexus in hypoxic hearts fails to make a connection to the aorta. In the normoxic specimen by ED9 (**A, C**), two coronary arteries with large lumen (arrows) are present, as well as numerous small vascular profiles on the anterior aspect of the ventricles (*). In the hypoxic heart with ventricular septal defect and decreased rotation of the great arteries, these vessels are absent (expected positions indicated by X), whereas the irregular plexus in the anterior interventricular sulcus is well formed. Ao, aorta; Pu, pulmonary trunk. Scale bar = 100 μm. **E–H**: higher power views of the ventricular wall showing rich microvasculature in the compact myocardium of both ventricles. There is an isolated capillary present in the trabeculae (Tr) of the hypoxic left ventricle (arrowhead). Note decreased thickness of the compact layer as well as trabeculae under hypoxia. The extent of the compact myocardium is indicated by double-sided arrows. LV, left ventricle; RV, right ventricle. Scale bar = 100 μm.

that apoptosis was similar under hypoxic and control conditions. In comparison between the right and left ventricle we observed a trend toward increased apoptosis in right ventricle in both normoxic ($P = 0.06$) and hypoxic condition ($P = 0.002$), similar to observations by others (Cheng et al., 2002). Analysis of sectioned hearts showed a mild increase of apoptosis under hypoxia. There were $15.4 \pm 8 \times 10^3$ positive cells per mm^3 of ventricular wall in the normoxic right ventricle versus $31.6 \pm 17 \times 10^3$ per mm^3 in the hypoxic right ventricle (mean $\pm$ SD, $P = 0.03$), and $13.05 \pm 4.4 \times 10^3$ in normoxic veruss $21.8 \pm 10.6 \times 10^3$ per mm^3 in the
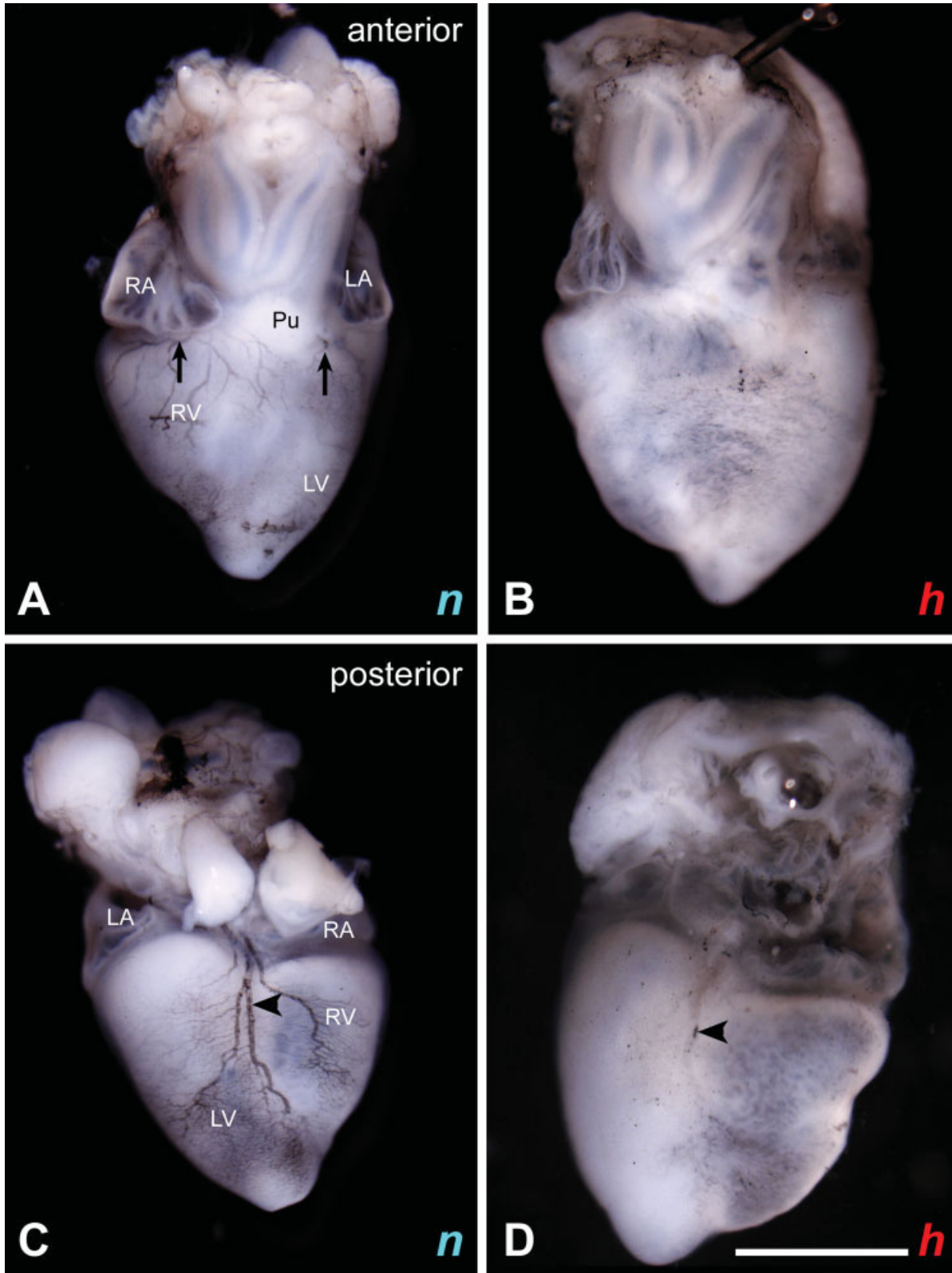
Fig. 6. Visualization of coronary vasculature by Indian ink injection in ED 9 (stage 37) normoxic (n) and hypoxic (h) embryos. LA, left atrium; RA, right atrium; LV, left ventricle; RV, right ventricle. Scale bar = 1 mm. **A, B**: Indian ink injection shows regular coronary arteries on the anterior (A) and posterior (B) surface of the normoxic heart. On the posterior aspect the ink fills the venous tree. The arrows on anterior aspect show the main coronary artery stems, arrowhead on the posterior aspect points to the cardiac venous plexus. **C, D**: Indian ink injection does not reveal regular coronary arteries on the anterior (C) and posterior (D) surface of the hypoxic heart. Panel C shows reduced right coronary artery suggesting its connection with aorta (arrow). Vascular plexus that had developed is not in the majority of cases connected to the aorta. The arrowhead on the posterior aspect shows the reduced venous plexus.
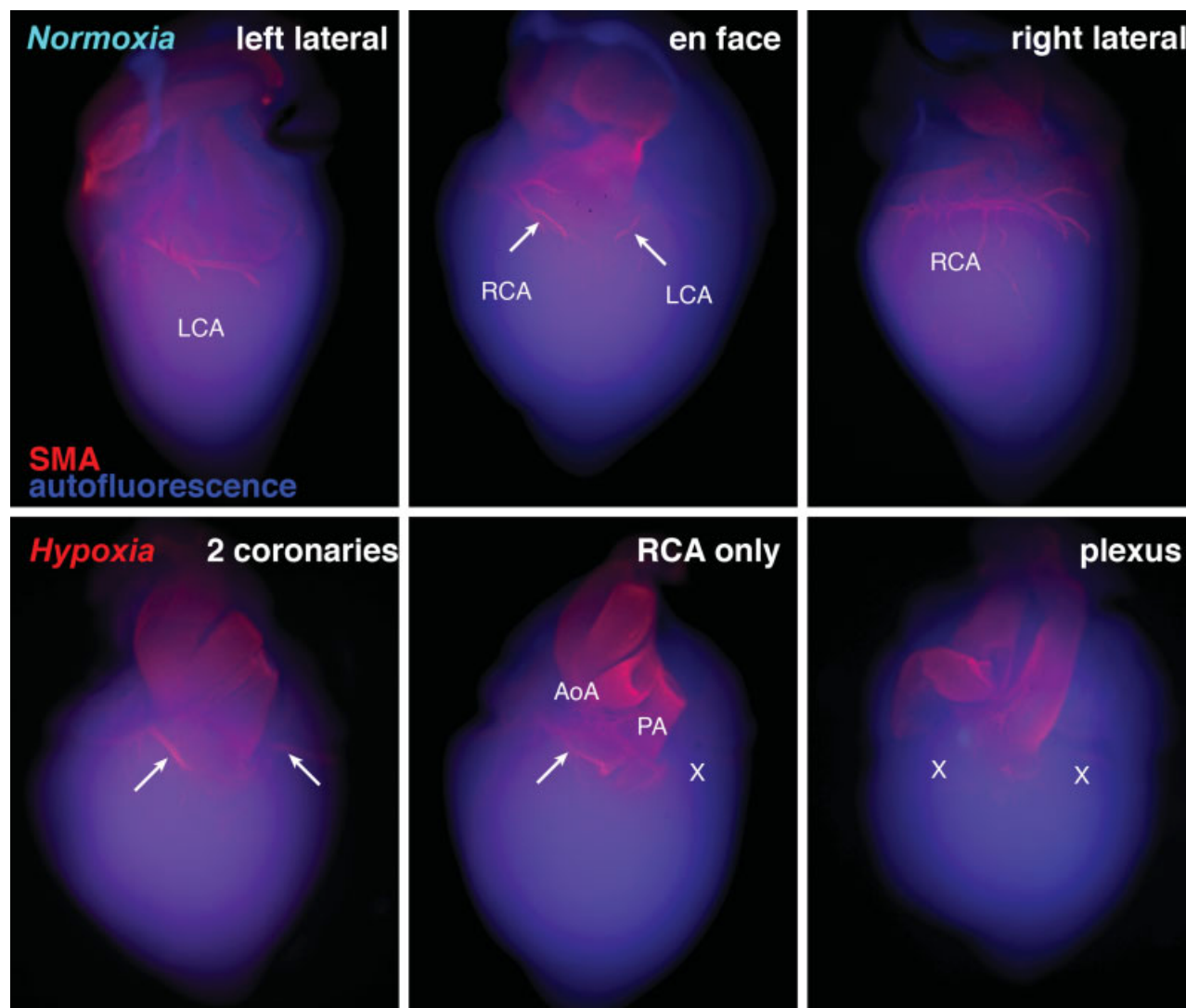
Fig. 7. Normal and abnormal coronary artery patterns in quail detected by whole mount SMA staining at ED9 (stage 37). In the normoxic heart (top row), two coronaries were regularly present. In hypoxic hearts (three different hearts shown in the bottom row), both normal pattern with two coronary arteries as well as absence of one (more often, as in this case, the left one) or both (right panel) coronaries were observed. Scale bar = 1 mm.

hypoxic left ventricle ($P = 0.14$). These results were confirmed by staining for active caspase-3, where we observed a similar mild (but statistically nonsignificant) increase under hypoxia. Similar trend with values below statistical significance was noted also on ED5 (stage 27/28) and ED6 (stage 29/30). Apoptosis data showed no appreciable increase in the myocardium (in agreement with Sedmera et al., 2002a) but increase in the subepicardium—during (deficient) rearrangement of vascular plexus into main tributaries.

DISCUSSION
Effect on Embryonic Survival

Hypoxia is a physiologic stimulus for vasculogenesis in development and pathology (Rouwet et al., 2002; Chan and Burggren, 2005). On the tissue level, hypoxia stimulates VEGF production via hypoxia-inducible factor (HIF) (Forsythe et al., 1996). Normal embryonic development requires VEGF levels within fairly narrow range, as both insufficiency (either heterozygosity for VEGF allele (Carmeliet et al., 1996) or inhibition via soluble antagonist (Drake et al., 2000) and excess (Feucht et al., 1997; Miquerol et al., 2000) result in severe vascular phenotype and early embryonic death. Phenotype of dead embryos in our model includes whole body edema (Nanka et al., 2006); it is difficult to determine whether this is primarily because of embryonic heart failure (due to ventricular noncompaction and dilation) or increased permeability of more abundant capillaries.

Abnormal Myocardial Development

Thin compact myocardium with more abundant trabeculation might present an adaptive mechanism compensating tissue-level hypoxia in the absence of coronary

TABLE 1. Incidence of coronary anomalies in ED8 and 9 (stages 34–35 and 37) hypoxic quail embryos

	16% O$_2$	21% O$_2$
Both coronary arteries—normal course	25%	97.5%
Only right coronary artery	30%	0%
Only left coronary artery	10%	2.5%
Irregular plexuses (no connection)	35%	0%

Results are based on analysis of 40 hearts per group.

arteries, rather than secondary dilation because of heart failure, since it is present from as soon as 3 days of hypoxic incubation (ED5, stage 27/28). Such increased trabeculation was previously described after experimentally increased VEGF levels (Feucht et al., 1997; Miquerol et al., 2000), as well as in the early stages of embryonic hypoxia in quail model in our previous paper (Nanka et al., 2006). Simultaneously, increased levels of VEGF stimulate proliferation of vascular precursors, leading to increased capillary density. Apparently, this is at the expense of myocyte proliferation, which is decreased under hypoxia. This corresponds to our unpublished findings of increased VEGF levels (together with increased capillary density, reported also in pathological literature) in the hypoplastic left ventricle. It was confirmed recently that even signaling through the same growth factor, fibroblast growth factor (FGF), is regulated by separate genetic cascades in myocardium (sonic hedgehog- and VEGF-independent) and coronary vasculature (Lavine et al., 2008). Interestingly, we found no hypoxia-induced differences in protein expression of another proangiogenic factor, FGF-2, in either myocardium or other areas of the embryo (unpublished observation). We cannot at present distinguish between primary myocardial cell-autonomous proliferative defect and dysregulation in signaling via growth factor(s) of epicardial origin (reviewed in Winter and Gittenberger-de Groot, 2007), which can also lead to thin compact myocardium. Epicardial-myocardial signaling is an active area of research, and recently, PDGF-A was identified as one (but the only) secreted factor of epicardial origin (Kang et al., 2008).

Expressing the proliferative index in cells per volume of tissue results in less time-consuming cell counting and validation by counting in one group (ED6) also the total number of cell nuclei showed that the values were within the range of 15%–50% of positive myocytes, comparable with our previous studies in the embryonic chick (Sedmera et al., 2002a; deAlmeida et al., 2007).

Apoptosis is a rare event in the developing ventricular myocardium and is considered a morphogenetic mechanism used for elimination of no longer needed subpopulations of myocytes in the AV region, outflow tract, and conduction system (Cheng et al., 2002; Sugishita et al., 2004). Unlike in the adult heart, embryonic ventricular cardiomyocytes show remarkable resistance to acute anoxia/reoxygenation (Sedmera et al., 2002b). The observed mild increase in cell death was concentrated predominantly in the subepicardium, and therefore more likely associated with impaired coronary vasculogenesis than compact layer thinning. This is in agreement with findings of more pronounced effect of hypoxia on compact
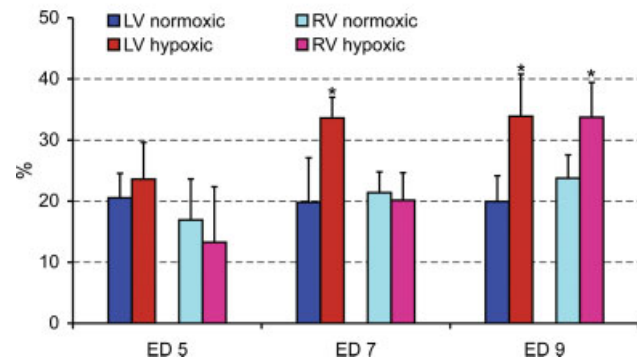

Fig. 8. Capillary density in right and left ventricular wall. The capillary density is increased under hypoxia, especially in the left ventricle. Mean ± SD, *$P < 0.05$ (t test). Embryonic days 5, 7, and 9 correspond to Hamburger-Hamilton stages 26/27, 31/32, and 37, respectively.

layer thickness in the left ventricle, which had less apoptotic cells that the right ventricle under both conditions.

Coronary Anomalies

As we have discussed earlier, both insufficiency (Carmeliet et al., 1996) and excess (Feucht et al., 1997) VEGF lead to abnormal vascular development. Impaired remodeling of coronary bed, especially deficient formation of two main coronary arteries penetrating to the aortic wall could be related to increased levels of VEGF, which is known to stimulate fusion of nascent capillary plexuses into large saccular vessels (Drake and Little, 1995; Miquerol et al., 2000). Absence of coronary arteries was reported in the quail model of inhibition of VEGF signaling using VEGF-trap (receptor 1 and 2 fusion protein) administered at ED6 or 7 (Tomanek et al., 2006b). Similar problem with connection of the coronary vessels to the aorta with resulting thin ventricular was reported in quail embryos with inhibited epicardial outgrowth (Eralp et al., 2005), but in that case, the problem was likely because of reduced number of subepicardial mesenchyme resulting from delayed epicardial covering of the heart. The connection of the coronary arteries to the aorta results in increased pressure in this part of the coronary vascular bed, which leads to recruitment of smooth muscle cells into arterial wall (Vrancken Peeters et al., 1997), so presence of smooth muscle coat around proximal portion of the coronary arteries can serve as a useful marker of their connection to the aorta (Tomanek et al., 2006a), as we found also in the present study.

Effect on Conduction System Maturation

Ventricular activation patterns observed in normoxic and hypoxic quail hearts were similar to those reported previously using the same optical mapping technique in the chick (Reckova et al., 2003), but the shift toward mature apex-to-base sequence appeared considerably sooner with first occurrence of this pattern present already at stage 23/ED4 vs. stage 31/ED7 in the chick. The patterns in hypoxia did not initially show any devia-
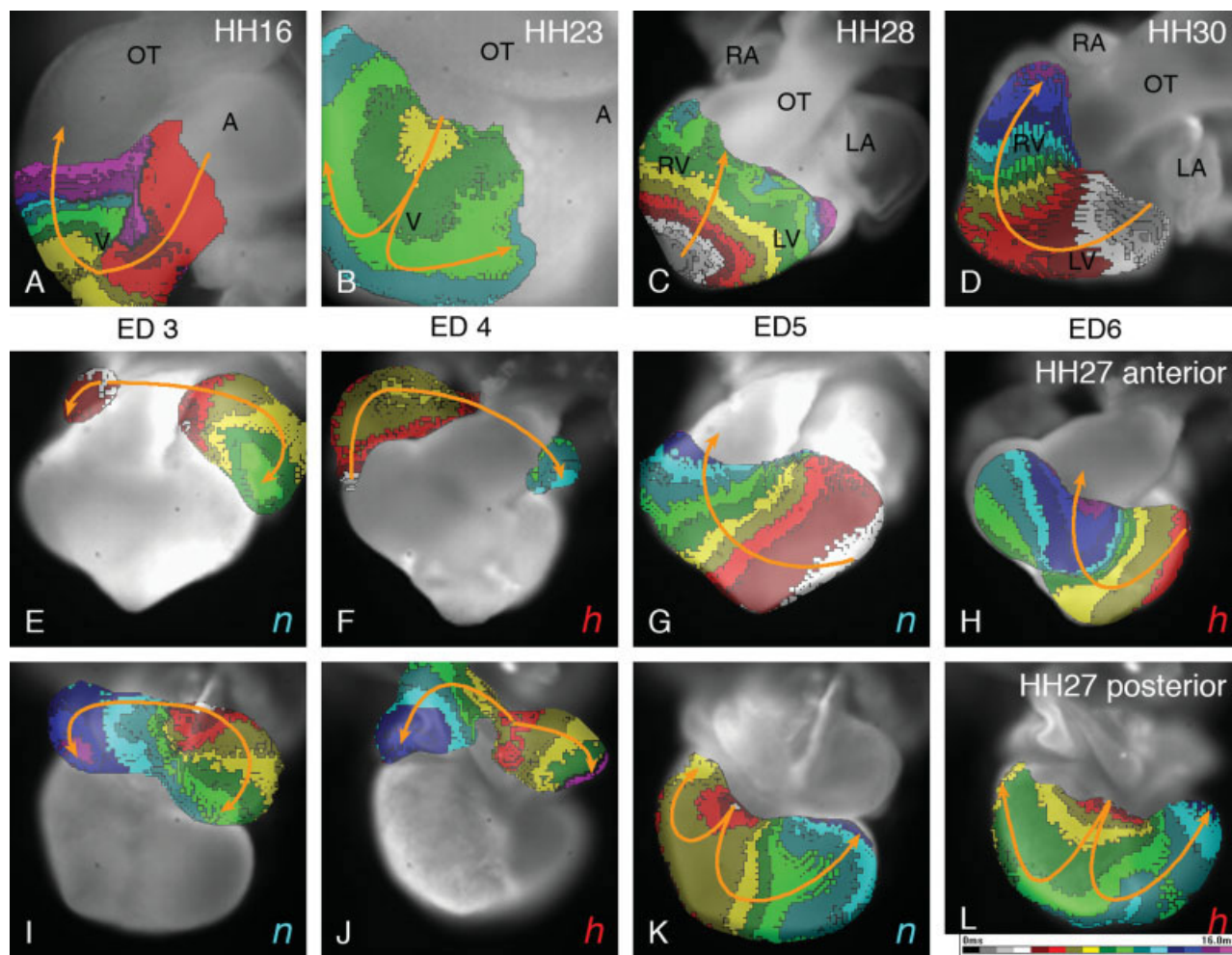
Fig. 9. Ventricular activation maps of normoxic and hypoxic quail hearts. **A–E**: illustration of typical activation patterns in frontal view at ED3, 4, 6, 7). Panel **A** shows peristaltoid-like wave of activation along the cardiac loop. Panel **B** is an example of an anterior activation pathway along the forming interventricular septum. Panel **C** illustrates apex-to-base activation observed sporadically from ED4. Panel **D** demonstrates that even at later stages, a significant proportion of hearts showed base-to-apex, left-to-right sweep of activation. **E–H**: anterior views of normoxic and hypoxic heart at ED5 showing separately atrial and ventricular activation. Note that there is no significant difference in location of atrial pacemaker or ventricular activation pattern. **I–L**: same hearts as above in posterior view show again similarity between normoxia and hypoxia. The atrial pacemaker is in both cases situated in the roof of the right atrium, and ventricles are activated from the left atrioventricular junction. In all figures, isochrones (also shown in color) are in 1 ms intervals and the direction of activation spread is indicated by orange arrows.

tion from the norm, but at the latest sampling interval (ED7) there was a clear acceleration of the normal process of conversion toward mature apex-to-base activation pattern (Chuck et al., 1997; Reckova et al., 2003). This may be due to slowing of ventricular myocyte proliferation, known to be associated with differentiation of ventricular conduction system (Cheng et al., 1999; Thompson et al., 2003) or increased endothelial signaling from hyperplastic, overstimulated endocardium (Gourdie et al., 1998; 2003) through molecules such as endothelin. To distinguish between these two possibilities, as well as to tease apart the nature of the myocardial proliferative defect, *in vitro* experiments would be necessary. Alternatively, recent study focused on development of fibrous insulation between the atria and ventricles (Kolditz et al., 2008) detailed the process of gradual disappear-

ance of muscular atrioventricular continuity, which is influenced by epicardial cells and can lead to abnormal base-to-apex activation patterns with ventricular preexcitation if perturbed experimentally. It is possible that just a slight increase in apoptosis in already hypoxic and cell death-prone myocardium of the atrioventricular canal that is also very sensitive to acute hypoxia (Sedmera et al., 2002b) could lead to a decrease in or accelerated disappearance of such connections, which would manifest as earlier appearance of mature apex-to-base activation patterns observed in ED7 hypoxic embryos in our study. However, as noted by Kolditz et al., there is little correlation between morphologically identifiable pathways and actual ventricular excitation patterns, so confirmation of this hypothesis would be challenging.

In conclusion, we have shown that hypoxic incubation of quail embryos during period of organogenesis leads to thin compact myocardium and impaired coronary vascularization that are consistent with elevated levels of VEGF. These changes are based on imbalance between myocardial and endocardial/endothelial proliferation, and coincide with accelerated conduction system maturation.

LITERATURE CITED

Bhattacharya S, Macdonald ST, Farthing CR. 2006. Molecular mechanisms controlling the coupled development of myocardium and coronary vasculature. Clin Sci (Lond) 111:35–46.

Carmeliet P, Ferreira V, Breier G, Pollefeyt S, Kieckens L, Gertsenstein M, Fahrig M, Vandenhoeck A, Harpal K, Eberhardt C, Declercq C, Pawling J, Moons L, Collen D, Risau W, Nagy A. 1996. Abnormal blood vessel development and lethality in embryos lacking a single VEGF allele. Nature 380:435–439.

Chan T, Burggren W. 2005. Hypoxic incubation creates differential morphological effects during specific developmental critical windows in the embryo of the chicken (Gallus gallus). Respir Physiol Neurobiol 145:251–263.

Cheng G, Litchenberg WH, Cole GJ, Mikawa T, Thompson RP, Gourdie RG. 1999. Development of the cardiac conduction system involves recruitment within a multipotent cardiomyogenic lineage. Development 126:5041–5049.

Cheng G, Wessels A, Gourdie RG, Thompson RP. 2002. Spatiotemporal distribution of apoptosis in embryonic chicken heart. Dev Dyn 223:119–133.

Chuck ET, Freeman DM, Watanabe M, Rosenbaum DS. 1997. Changing activation sequence in the embryonic chick heart. Implications for the development of the His-Purkinje system. Circ Res 81:470–476.

Chuck ET, Watanabe M. 1997. Differential expression of PSA-NCAM and HNK-1 epitopes in the developing cardiac conduction system of the chick. Dev Dyn 209:182–195.

deAlmeida A, McQuinn T, Sedmera D. 2007. Increased ventricular preload is compensated by myocyte proliferation in normal and hypoplastic fetal chick left ventricle. Circ Res 100:1363–1370.

Drake CJ, LaRue A, Ferrara N, Little CD. 2000. VEGF regulates cell behavior during vasculogenesis. Dev Biol 224:178–188.

Drake CJ, Little CD. 1995. Exogenous vascular endothelial growth factor induces malformed and hyperfused vessels during embryonic neovascularization. Proc Natl Acad Sci USA 92:7657–7661.

Eralp I, Lie-Venema H, DeRuiter MC, van den Akker NM, Bogers AJ, Mentink MM, Poelmann RE, Gittenberger-de Groot AC. 2005. Coronary artery and orifice development is associated with proper timing of epicardial outgrowth and correlated Fas-ligand-associated apoptosis patterns. Circ Res 96:526–534.

Feucht M, Christ B, Wilting J. 1997. VEGF induces cardiovascular malformation and embryonic lethality. Am J Pathol 151:1407–1416.

Forsythe JA, Jiang BH, Iyer NV, Angani F, Leung SW, Koos RD, Semenza GL. 1996. Activation of vascular endothelial growth factor gene transcription by hypoxia-inducible factor 1. Mol Cell Biol 16:4604–4613.

Gourdie RG, Harris BS, Bond J, Edmondson AM, Cheng G, Sedmera D, O'Brien TX, Mikawa T, Thompson RP. 2003. His-Purkinje lineages and development. Novartis Found Symp 250:110–122; discussion 122–114, 276–119.

Gourdie RG, Wei Y, Kim D, Klatt SC, Mikawa T. 1998. Endothelin-induced conversion of embryonic heart muscle cells into impulse-conducting Purkinje fibers. Proc Natl Acad Sci USA 95:6815–6818.

Hamburger V, Hamilton HL. 1951. A series of normal stages in the development of the chick embryo. J Morphol 88:49–92.

Jaffee OC. 1978. Hemodynamics and cardiogenesis: the effects of physiologic factors on cardiac development. Birth Defects: Orig Artic Ser 14:393–404.

Kang J, Gu Y, Li P, Johnson BL, Sucov HM, Thomas PS. 2008. PDGF-A as an epicardial mitogen during heart development. Dev Dyn 237:692–701.

Kolditz DP, Wijffels MC, Blom NA, van der Laarse A, Hahurij ND, Lie-Venema H, Markwald RR, Poelmann RE, Schalij MJ, Gittenberger-de Groot AC. 2008. Epicardium-derived cells in development of annulus fibrosis and persistence of accessory pathways. Circulation 117:1508–1517.

Kwee L, Baldwin HS, Shen HM, Stewart CL, Buck C, Buck CA, Labow MA. 1995. Defective development of the embryonic and extraembryonic circulatory systems in vascular cell adhesion molecule (VCAM-1) deficient mice. Development 121:489–503.

Lavine KJ, Schmid GJ, Smith CS, Ornitz DM. 2008. Novel tool to suppress cell proliferation in vivo demonstrates that myocardial and coronary vascular growth represent distinct developmental programs. Dev Dyn 237:713–724.

Miquerol L, Langille BL, Nagy A. 2000. Embryonic development is disrupted by modest increases in vascular endothelial growth factor gene expression. Development 127:3941–3946.

Nanka O, Valasek P, Dvorakova M, Grim M. 2006. Experimental hypoxia and embryonic angiogenesis. Dev Dyn 235:723–733.

Olivey HE, Compton LA, Barnett JV. 2004. Coronary vessel development: the epicardium delivers. Trends Cardiovasc Med 14:247–251.

Pardanaud L, Altmann C, Kitos P, Dieterlen-Lievre F, Buck CA. 1987. Vasculogenesis in the early quail blastodisc as studied with a monoclonal antibody recognizing endothelial cells. Development 100:339–349.

Reckova M, Rosengarten C, deAlmeida A, Stanley CP, Wessels A, Gourdie RG, Thompson RP, Sedmera D. 2003. Hemodynamics is a key epigenetic factor in development of the cardiac conduction system. Circ Res 93:77–85.

Ribatti D. 2006. Genetic and epigenetic mechanisms in the early development of the vascular system. J Anat 208:139–152.

Rouwet EV, Tintu AN, Schellings MW, van Bilsen M, Lutgens E, Hofstra L, Slaaf DW, Ramsay G, Le Noble FA. 2002. Hypoxia induces aortic hypertrophic growth, left ventricular dysfunction, and sympathetic hyperinnervation of peripheral arteries in the chick embryo. Circulation 105:2791–2796.

Rychter Z, Ostadal B. 1971. Fate of "sinusoidal" intertrabecular spaces of the cardiac wall after development of the coronary vascular bed in chick embryo. Folia Morphol 19:31–44.

Rychterova V. 1971. Principle of growth in thickness of the heart ventricular wall in the chick embryo. Folia Morphol (Praha) 19:262–272.

Schaefer KS, Doughman YQ, Fisher SA, Watanabe M. 2004. Dynamic patterns of apoptosis in the developing chicken heart. Dev Dyn 229:489–499.

Sedmera D, Hu N, Weiss KM, Keller BB, Denslow S, Thompson RP. 2002a. Cellular changes in experimental left heart hypoplasia. Anat Rec 267:137–145.

Sedmera D, Kucera P, Raddatz E. 2002b. Developmental changes in cardiac recovery from anoxia-reoxygenation. Am J Physiol Regul Integr Comp Physiol 283:R379–R388.

Sedmera D, Pexieder T, Vuillemin M, Thompson RP, Anderson RH. 2000. Developmental patterning of the myocardium. Anat Rec 258:319–337.

Sedmera D, Reckova M, Bigelow MR, DeAlmeida A, Stanley CP, Mikawa T, Gourdie RG, Thompson RP. 2004. Developmental transitions in electrical activation patterns in chick embryonic heart. Anat Rec A 280:1001–1009.

Sedmera D, Wessels A, Trusk TC, Thompson RP, Hewett KW, Gourdie RG. 2006. Changes in activation sequence of embryonic chick atria correlate with developing myocardial architecture. Am J Physiol Heart Circ Physiol 291:H1646–H1652.

Sharma SK, Lucitti JL, Nordman C, Tinney JP, Tobita K, Keller BB. 2006. Impact of hypoxia on early chick embryo growth and cardiovascular function. Pediatr Res 59:116–120.

Sugishita Y, Watanabe M, Fisher SA. 2004. Role of myocardial hypoxia in the remodeling of the embryonic avian cardiac outflow tract. Dev Biol 267:294–308.

Thompson RP, Reckova M, DeAlmeida A, Bigelow M, Stanley CP, Spruill JB, Trusk T, Sedmera D. 2003. The oldest, toughest cells in the heart. In: Chadwick DJ, Goode J, editors. Development of the cardiac conduction system. Chichester: Wiley. p 157–176.

Tomanek RJ, Hansen HK, Dedkov EI. 2006a. Vascular patterning of the quail coronary system during development. Anat Rec A Discov Mol Cell Evol Biol 288:989–999.

Tomanek RJ, Ishii Y, Holifield JS, Sjogren CL, Hansen HK, Mikawa T. 2006b. VEGF family members regulate myocardial tubulogenesis and coronary artery formation in the embryo. Circ Res 98:947–953.

Varnava AM. 2001. Isolated left ventricular non-compaction: a distinct cardiomyopathy? Heart 86:599–600.

Viragh S, Gittenberger-de Groot AC, Poelmann RE, Kalman F. 1993. Early development of quail heart epicardium and associated vascular and glandular structures. Anat Embryol (Berl) 188:381–393.

Vrancken Peeters MP, Gittenberger-de Groot AC, Mentink MM, Hungerford JE, Little CD, Poelmann RE. 1997. The development of the coronary vessels and their differentiation into arteries and veins in the embryonic quail heart. Dev Dyn 208:338–348.

Vrancken Peeters MP, Gittenberger-de Groot AC, Mentink MM, Poelmann RE. 1999. Smooth muscle cells and fibroblasts of the coronary arteries derive from epithelial-mesenchymal transformation of the epicardium. Anat Embryol (Berl) 199:367–378.

Webster WS, Abela D. 2007. The effect of hypoxia in development. Birth Defects Res C Embryo Today 81:215–228.

Wessels A, Sedmera D. 2003. Developmental anatomy of the heart: a tale of mice and man. Physiol Genomics 15:165–176.

Wikenheiser J, Doughman YQ, Fisher SA, Watanabe M. 2006. Differential levels of tissue hypoxia in the developing chicken heart. Dev Dyn 235:115–123.

Winter EM, Gittenberger-de Groot AC. 2007. Epicardium-derived cells in cardiogenesis and cardiac regeneration. Cell Mol Life Sci 64:692–703.